THE JOURNAL OF BIOLOGICAL CHEMISTRY VOL. 289, NO. 31, pp. 21401–21412, August 1, 2014

Calcineurin-mediated YB-1 Dephosphorylation Regulates CCL5 Expression during Monocyte Differentiation*

Received for publication, March 6, 2014, and in revised form, June 13, 2014 Published, JBC Papers in Press, June 19, 2014, DOI 10.1074/jbc.M114.562991

Christina Alidousty[‡1], Thomas Rauen[‡1], Lydia Hanssen[‡], Qiang Wang[§], Setareh Alampour-Rajabi[¶], Peter R. Mertens[‖], Jürgen Bernhagen[¶2], Jürgen Floege[‡3], Tammo Ostendorf[‡3], and Ute Raffetseder[‡4]

From the [‡]Department of Nephrology and Clinical Immunology, University Hospital RWTH-Aachen, Pauwelsstrasse 30, 52057 Aachen, Germany, the [§]Department of Rheumatology, First Affiliated Hospital of Nanjing Medical University, Nanjing, Jiangsu 210029, China, the [¶]Department of Cell and Molecular Biology, Institute of Biochemistry and Molecular Cell Biology, University Hospital RWTH-Aachen, Pauwelsstrasse 30, 52057 Aachen, Germany, and the [‖]Department of Nephrology, Hypertension, Diabetes, and Endocrinology, Otto-von-Guericke-University, 39120 Magdeburg, Germany

Background: Transcription factor YB-1 constitutes a key regulator in immune cell homeostasis. It has been demonstrated to be involved in monocyte/macrophage differentiation. However, the underlying mechanisms are poorly understood.
Results: Protein phosphatase calcineurin (CN) regulates YB-1 activities on the *CCL5* promoter during macrophage differentiation.
Conclusion: Dephosphorylation of YB-1 by CN is crucial to counteract the overwhelming pro-inflammatory propensities of YB-1.
Significance: Overshooting inflammation may be counteracted by dephosphorylation of YB-1.

Y-box (YB) protein-1 serves as a master regulator in gene transcription and mRNA translation. YB-1 itself is regulated at various levels, *e.g.* through post-translational modifications. In our previous work, we identified RANTES/CCL5 as a transcriptional target of YB-1. We previously demonstrated that YB-1 protein is transiently up-regulated during monocyte/macrophage differentiation evidenced in monocytic cells (THP-1 cells) that were differentiated using phorbol myristate acetate (PMA). Here we provide evidence that YB-1 phosphorylation, specifically at its serine residue 102 (Ser-102), increases early on in THP-1 cells following PMA treatment as well as in differentiated primary human monocytes. This process is mediated through the Akt signaling pathway. Ser-102-phosphorylated YB-1 displays stronger binding affinity and *trans*-activating capacity at the *CCL5* gene promoter. Notably, Ser-102-phosphorylated YB-1 disappears at later stages of the monocyte/macrophage differentiation process. We demonstrate that serine-threonine phosphatase calcineurin (CN) dephosphorylates YB-1 preventing it from binding to and *trans*-activating the *CCL5* promoter. Co-immunoprecipitation assays prove a direct YB-1/CN interaction. Furthermore, analyses in kidney tissues from mice that were treated with the CN inhibitor cyclosporine A revealed an *in vivo* effect of CN on the YB-1 phosphorylation status. We conclude that YB-1 phosphorylation at Ser-102 is an important prerequisite for *CCL5* promoter activation during macrophage differentiation. Our findings point to a critical role of YB-1 in the resolution of inflammatory processes which may largely be due to CN-mediated dephosphorylation.

Post-translational modifications of proteins increase the functional diversity of the proteome by covalent addition of functional groups. Phosphorylation and dephosphorylation are the most common protein modifications and crucially contribute to the fine-tuning of multiple biological processes that are often accompanied by intracellular translocation of the respective proteins (1, 2).

Calcineurin (CN),[5] also known as protein phosphatase 2B (PP2B), constitutes a calcium-dependent serine-threonine (Ser/Thr) phosphatase. In response to increased intracellular calcium levels, CN dephosphorylates and thereby activates transcription factors including nuclear factor of activated T cells (NFAT). In a complex together with CN, NFAT shuttles into the nucleus and induces gene transcription, *e.g.* that of interleukin (IL)-2 (3, 4). This signal transduction pathway was initially characterized in T lymphocytes. In these cells, CN inhibitors (CNIs), such as cyclosporine A (CsA) and tacrolimus (FK506), can efficiently block CN effects at various stages in the immune system. CN has evolved as a major target of immunosuppressant drugs and CNIs are an integral part of standard therapy regimens to prevent allograft rejection (5, 6). However, despite the beneficial effects on allograft survival, CNIs also exert nephrotoxic side effects contributing to acute or chronic allograft nephropathy (7). Recent findings from our group point

* This work was funded by the Fritz-Bender-Stiftung (to T. R. and U. R.), START-Program (Faculty of Medicine, RWTH, Aachen, to T. R. and U. R.), SFB/TRR57 (to T. O. and J. F.), SFB854 and Me1365/7-1 (to P. R. M.) and SFB 542 projects C12 (to U. R. and P. R. M.).
[1] Both authors contributed equally to this work.
[2] Recipient of funding from DFG Projects SFB-TRR57/A07 and FOR809/TP1-Be1977/4-2.
[3] Recipient of funding from the Interdisciplinary Center for Clinical Research (IZKF) within the Faculty of Medicine at the RWTH Aachen University (E6-10).
[4] To whom correspondence should be addressed: Department of Nephrology and Clinical Immunology, RWTH Aachen University Hospital, Pauwelsstrasse 30, 52057 Aachen, Germany. Tel.: 49-241-8088213; Fax: 49-241-8082446; E-mail: uraffetseder@ukaachen.de.

[5] The abbreviations used are: CN, calcineurin; YB, Y-box; PMA, phorbol myristate acetate; NFAT, nuclear factor of activated T cells; CNI, CN inhibitor; CsA, cyclosporine A.

to profibrotic properties of Y-box protein-1 (YB-1) in CNI-challenged mesangial cells (MCs) (8).

YB-1 is a highly conserved protein that has been shown to associate with DNA elements encompassing inverted CAATT-box sequences (Y-boxes) as well as with RNA in the cytoplasm. By this, YB-1 is involved in the regulation of DNA transcription (9, 10), RNA splicing (11) and translational control of protein synthesis (8, 12). *In vitro* analysis in MCs revealed a severalfold induction of cellular YB-1 protein content upon CsA treatment that resulted in stabilization and generation of type 1 collagen (*Col1A*) mRNA (8). Whether CN can act directly on the YB-1 activity by dephosphorylation of the protein is unknown. Although there is growing knowledge of how YB-1 is phosphorylated (13, 14), little is known about its dephosphorylation processes. The Ser/Thr phosphatase PP2Cγ is involved in spliceosome assembly and has been shown to interact with YB-1 (15); however, a subsequent change in the phosphorylation state of YB-1 has not been investigated so far. *In vivo* and *ex vivo* data demonstrate that YB-1 is post-translationally phosphorylated at amino acid position 102 (serine 102 (Ser-102)) at the onset of lipopolysaccharide (LPS)-triggered inflammation (16). However, this modification is no longer detectable during the late phase of inflammation, pointing to a reversible phosphorylation of YB-1 (16).

We have previously demonstrated a pivotal regulatory role for YB-1 in *CCL5*/*RANTES* gene transcription by binding to its specific gene promoter in transplant rejection (17) and atherogenesis (18). Chemokines such as CCL5 permit monocytes to infiltrate the tissue and propagate a process denoted "differentiation" into macrophages (19, 20). YB-1 has the potential to initiate and later on to abate the inflammation process as it activates CCL5 expression in monocytes. However, upon macrophage differentiation, it accomplishes *trans*-repressive capacities on the *CCL5* promoter (17). The appearance of a high mobility complex in YB-1-DNA binding studies indicated that partnering with other proteins on the Y-box of the *CCL5* promoter occurs during the macrophage differentiation process (21). These results prompted us to hypothesize that CN could be involved in this process. CN has the capacity to translocate to the nucleus (22, 23) and by this, it may mediate the repressive effect on *CCL5* gene transcription in macrophages by dephosphorylation of YB-1.

To identify the molecular mechanisms behind YB-1 action during monocyte differentiation, we first studied YB-1 phosphorylation, translocation, and gene transcription in the phorbol myristate acetate (PMA)-triggered monocyte differentiation model and in primary human monocytes/macrophages and then investigated the interplay between CN and YB-1 in the context of *CCL5* promoter activation.

EXPERIMENTAL PROCEDURES

Cell Culture—Human monocytes (THP-1) and rat mesangial cells (rMCs) were cultured in RPMI 1640, and human embryonic kidney cells (HEK293T) were grown in Dulbecco's modified Eagle's medium (DMEM, low glucose). Media and supplements (10% FCS, 100 units/ml penicillin, 100 μg/ml streptomycin) were purchased from Invitrogen. All cell lines were maintained in humidified air with 5% CO_2 content at 37 °C.

For induction of YB-1 phosphorylation, rMCs (1×10^6) or HEK293T cells (2×10^6) were seeded in 75 cm^2 cell culture flasks and grown in serum-reduced media with 1% FCS 24 h prior to challenge. Cells were stimulated for 1 h with 100 ng/ml recombinant human epidermal growth factor (EGF) (Immunotools) or rat insulin-like growth factor (IGF) (Prospec), respectively. To prevent PMA-induced phosphorylation of YB-1, THP-1 cells were preincubated either with 10 μM Ly294002 (Calbiochem) or 38 μM SL0101 (Calbiochem). To induce monocyte differentiation, 1×10^7 THP-1 cells were incubated with 100 nM PMA (Sigma-Aldrich) for the indicated periods.

Plasmids—Plasmids encoding for *CCL5* promoter fused to the luciferase gene have been described previously (17). A full-length YB-1 expression plasmid (YB-1-pSG5) was kindly donated by J. Ting (Lineberger Comprehensive Center, University of North Carolina) (24). For immunofluorescence studies, an expression plasmid was used that encodes the full-length YB-1 protein with a C-terminal CFP-tag (pDREAM vector, Genscript). A pEYFP-N2 N-terminal protein fusion vector containing a CN-encoding DNA fragment was kindly donated by M. L. Dell'Acqua and W. A. Sather. Overexpression of CN in different cell lines was performed using a pEGFP-C3-CNAbeta expression plasmid (donated by Oliver Ritter, Ref. 23).

Transient Transfections—Transient transfections in HEK293T cells were performed using calcium phosphate precipitates as described previously (25). rMCs (2×10^6) were transfected with the lipid-based transfection reagent Fugene HD (Promega) according to the manufacturer's instructions. Human THP-1 cells were transfected through electroporation. Briefly, 1×10^7 non-adherent cells were pelleted and resuspended in 1 ml of RPMI 1640 medium supplemented with 20% FCS. Next, 2.5×10^6 cells (250 μl) were added to electroporation cuvettes (0.4 cm gap, Bio-Rad) together with a total amount of 20 μg plasmid DNA, respectively. The mixture was incubated for 5 min on ice and THP-1 cells were electroporated at 250 V/1100 μF in a Gene Pulser II electroporation system (Bio-Rad). Cells were incubated another 5 min on ice prior to resuspension in 2 ml of RPMI 1640 medium supplemented with 20% FCS, transferred to 6-well tissue culture plates and incubated at 37 °C and 5% CO_2 for 6/24 h.

Preparation of Whole Cell Lysates, Nuclear, and Cytoplasmic Cell Extracts and Immunoblotting—For preparation of whole cell lysates, cells were harvested, washed once with ice-cold PBS, and lysed with 1 ml RIPA buffer (50 mM Tris-HCl, pH 7.4, 1% Nonidet P-40, 0.25% sodium deoxycholate, 150 mM NaCl, 1 mM EDTA, 1 mM sodium orthovanadate, protease inhibitors, phosphatase inhibitors (Roche Applied Science)). After 30-min incubation on ice, lysates were centrifuged (15 min, 4 °C, 14,000 rpm), and supernatants were collected and stored at −80 °C.

For preparation of nuclear and cytoplasmic cell extracts, 1×10^7 THP-1 or 2×10^6 HEK293T cells were grown in tissue culture dishes, washed with ice-cold PBS, pelleted and resuspended in 200 μl of hypotonic buffer A (10 mM HEPES-KOH 7.9, 1.5 mM $MgCl_2$, 10 mM KCl, 0.5 mM DTT, 1 mM sodium orthovanadate, protease inhibitors (Roche Applied Science)). After 10 min of incubation on ice, samples were vortexed for

10 s and the cell nuclei pelleted by centrifugation (5 min, 2,000 rpm, 4 °C). Supernatants (cytoplasmatic fractions) were harvested and frozen at −80 °C. Nuclear pellets were washed five times with buffer A and resuspended in 50 μl of buffer C (20 mM HEPES-KOH pH 7.9, 1.5 mM $MgCl_2$,420 mM NaCl, 0.2 mM EDTA, 25% glycerol, 0.5 mM DTT, 1 mM sodium orthovanadate, protease inhibitors). After 20 min of incubation on ice, the supernatants containing nuclear proteins were collected by spinning at 14,000 rpm (5 min, 4 °C).

Nuclear and cytoplasmic cell extracts of kidney tissue were prepared as follows: ~50 μg of minced kidneys were lysed with 400 μl of buffer A, homogenized and sonicated (3 times, 10 s each cycle). The suspension was incubated for 10 min on ice and nuclei pelleted by centrifugation (5 min, 2,000 rpm, 4 °C). The cytoplasmic fraction was collected and nuclear protein extracts prepared as described above.

Protein concentrations were determined by the BCA protein assay (Interchim), using bovine serum albumin as a standard. Extracts were stored at −80 °C until 10–30 μg of lysates were subjected to SDS-polyacrylamide gel electrophoresis. Proteins were transferred to a nitrocellulose membrane and detected using Lumi-Light/Lumi-Light^{PLUS} Western blotting Substrate (Roche Applied Science) with the following antibodies: YB-1 (polyclonal antibody against protein C terminus, Sigma), phospho-YB-1 (monoclonal antibody against phosphorylated Ser-102, Cell Signaling), calcineurin (polyclonal antibody against calcineurin A, Cell Signaling), Akt (polyclonal antibody against Akt kinase, Cell Signaling), histone H3 (monoclonal antibody against histone H3 (3H1), Cell Signaling). To ensure equal protein loading of whole cell lysates or cytoplasmatic extracts, blots were incubated with a monoclonal GAPDH-specific antibody (Novus Biologicals), whereas a CREB-specific antibody (Cell Signaling) was used for nuclear extracts. Band intensities were quantified by the Image J software, and after normalization against values determined for GAPDH/CREB, the p-YB-1 content was set as 1, and relative band intensities were calculated.

Immunofluorescence and Confocal Microscopy—The 2×10^5 HEK293T cells were plated on poly-L-lysine-coated coverslips in 6-well plates 1 day prior to transfection with YB-1-CFP-expressing vector. Twenty-four hours after transfection, the cells were stimulated for 1 h with IGF as described above, washed twice with PBS, fixed with 4% paraformaldehyde (30 min, 37 °C) and washed again two times with PBS and once with water. Coverslips were mounted with Immu-Mount (Thermo Scientific). Confocal laser scanning microscopy (Zeiss LSM 710 confocal microscope, Zeiss, Jena, Germany) was performed at 405 nm for CFP fluorescence (detected at 454 nm $< \lambda_{CFP} <$ 515 nm).

ELISAs—To quantify the secreted CCL5 protein content in the cell culture medium of THP-1 cells, the quantitative sandwich enzyme immunoassay technique with reagents from R&D Systems (Minneapolis, MN; DuoSet ELISA development kit DY278) was performed according to the manufacturer's instructions. The optical density was measured using a microplate reader set to 450 nm. All standards and samples were assayed as duplicates of at least three independent experiments.

Chromatin Immunoprecipitations (ChIPs)—ChIP assays were performed using the Chromatin Immunoprecipitation Assay Kit from Millipore according to the manufacturer's protocol. 1×10^7 THP-1 cells were seeded in 10-cm dishes and cross-linked with 1% formaldehyde in tissue culture medium for 10 min at 37 °C. Cell samples were washed twice in ice-cold phosphate-buffered saline containing protease inhibitors (1 Protease Inhibitor Mixture Tablet (Roche Applied Science) dissolved in 50 ml PBS). Cells were lysed in SDS lysis buffer. Samples were sonicated to shear DNA and incubated with a p-YB-1-specific antibody (Cell Signaling) or IgG as negative control (Millipore) overnight at 4 °C. A proportion (20%) of the samples was kept as "input" to represent the PCR amplification of the total sample. Immune complexes were precipitated with ChIP-grade Protein A/G Plus-agarose (Thermo Scientific). DNA was prepared by incubation with proteinase K enzyme (Roche Applied Science) for 1 h at 45 °C, recovered using a QIAamp DNA Mini Kit protocol (Qiagen) and subjected to real-time PCR analysis.

The real-time qPCR primer sequences used to amplify the regions within the *CCL5* gene locus were as follows: 5′-CTCTGAGGAGGACCCCTTCC-3′; 5′-TTCCTCTTTGACCAAGCACCA-3′.

The amount of immunoprecipitated DNA was subtracted by the amplified DNA that was bound by the nonspecific IgG antibody and calculated relative to the respective input DNA. Further, real-time qPCR products were separated on 2% agarose gel stained with GelRed (Biotium).

Luciferase Assays—THP-1 cells were transfected by electroporation as described above including 10 ng of *Renilla* luciferase control plasmid per transfection. At 6/24 h after electroporation, the cells were harvested and lysed with 50 μl of passive lysis buffer. After incubation for 15 min on ice and centrifugation (5 min, 14,000 rpm, 4 °C) lysates were assayed for luciferase activity using the Dual-Luciferase® Assay System (Promega) following the manufacturer's instructions on a Sirius luminometer (Berthold Detection Systems). *Renilla* luciferase activity was measured to control for transfection efficiency. Results were confirmed in at least three independent experiments and calculated as fold changes relative to luciferase activity measured with *CCL5* promoter plasmid.

Electrophoretic Mobility Shift Analyses—Biotin 3′-end labeling of synthetic DNA probes corresponding to the antisense strands of the *CCL5* promoter sequences was performed as described previously (17). Biotin-labeled DNA was incubated with nuclear cell extract for 20 min at room temperature, subjected to electrophoresis on native 6% polyacrylamide gels, and transferred to nylon membranes. The bands were visualized by streptavidin horseradish peroxidase conjugate and chemiluminescent substrate (Light-Shift chemiluminescent EMSA kit, Pierce).

For supershift analyses, the following antibodies were incubated with nuclear proteins 20 min prior to addition of probes: IgG as negative control (Millipore), polyclonal anti-calcineurin, polyclonal anti-Akt, and p-YB-1-specific antibody (all obtained from Cell Signaling). Supershifted complexes were indirectly deduced from decreased band intensities on the retardation gels, whereas bands should not change when control IgGs were added to the binding reactions. The binding reaction was per-

formed as described above, and samples were subjected to electrophoresis on 6% polyacrylamide gels.

Co-immunoprecipitation of CN Associated with YB-1—Prior to immunoprecipitation, polyclonal anti-calcineurin antibody (Cell Signaling) and nonspecific rabbit IgG (Santa Cruz Biotechnology) as negative control were covalently linked to protein A-Sepharose beads (50% suspension; Invitrogen), as described before (16). A total of 40 μl of protein A-Sepharose coupled with either polyclonal CN antibody or nonspecific IgG was incubated with 200 μg of total cell extracts or cytoplasmic (200 μg) and nuclear (100 μg) protein extracts from HEK293T cells, respectively, for 90 min at 4 °C in immunoprecipitation buffer (20 mM HEPES, 100 mM potassium chloride, 5 mM magnesium acetate, 1 mM DTT, 0.025% Triton X-100, and protease inhibitors). Sepharose beads were washed six times in immunoprecipitation buffer and one time in PBS buffer, and precipitated material was resuspended in 50 μl of Western blot sample buffer. Then 10 μl of samples were subjected to SDS-polyacrylamide gel electrophoresis.

Quantitative Real-time PCR—For quantitative real-time PCR (qRT-PCR), 1.25×10^7 THP-1 cells were transfected with either a CN-GFP or GFP control plasmid by means of electroporation as described above and cultured in RPMI 1640 medium supplemented with 20% FCS for 6 or 24 h, respectively. Total RNA was purified using a my-Budget RNA Mini Kit (Bio-Budget) according to the manufacturer's protocol. First-strand cDNA was synthesized with Moloney-monkey leukemia virus reverse transcriptase (Invitrogen). qRT-PCR was carried out on the 7300 real-time PCR system (Applied Biosystems). TaqMan master mix and TaqMan primer sets were obtained for human CCL5 (Hs00174575_m1), human CN (Hs00917458_m1), and eukaryotic 18 S rRNA (Hs99999901_s1) as an internal control from Applied Biosystems. Results were calculated using the comparative deltaCT methodology. For ChIP analyses, real-time qPCR was performed using a SYBR Green PCR kit (Eurogentec, Cologne, Germany).

Chronic CsA Nephropathy in Vivo—Animals were housed in cages with constant temperature and humidity and drinking water and food *ad libitum*. The local review board approved this animal experiment according to prevailing guidelines for scientific animal experimentation. One week prior to and during the experiments animals received a low salt diet with distilled water *ad libitum*. Female 16-week-old C57BL/6 mice (The Jackson Laboratory, Bar Harbor, ME) with a weight of 20–24 g received daily subcutaneous injections of 30 mg/kg of CsA (Sandimmune®, Novartis) or identical volume of the vehicle (27% Cremophor® EL, 33% ethanol and 40% of a 0.9% NaCl solution) as control. After 5 weeks, the animals were sacrificed, and kidneys were removed and frozen on dry ice for protein extraction. Extraction of nuclear and cytoplasmic extracts from renal tissues was performed as described previously.

Isolation of Primary Human Monocytic Cells and FACS Analysis—Human peripheral blood mononuclear cells from pooled samples obtained from three healthy blood donors of the local blood bank were isolated by density gradient centrifugation by means of buffy coats. CD14-positive monocytes were isolated by immunomagnetic separation (MACS; Miltenyi Biotec) according to the manufacturer's instructions. Separated cells were analyzed fresh (day 0) or resuspended in RPMI 1640 containing 5% human serum to allow cells to adhere and differentiate for 24 h at 37 °C. Nuclear and cytoplasmic cell extracts were prepared as described above. Western blot analyses from these samples were run in three independent experimental approaches.

Effective differentiation process was assessed by surface expression of ICAM-1/CD54 as a macrophage marker molecule through FACS analysis. Briefly, 3×10^5 cells were washed with PBS supplemented with 0.5% BSA and 0.1% sodium azide and stained with a fluorescein-conjugated anti-CD54 antibody (R&D Systems). Specificity of staining was confirmed using the corresponding isotype control. Stained cells were washed and analyzed on a FACSCanto II (BD Biosciences). Measurements were quantified using FlowJo software (TreeStar, Ashland, OR).

Statistical Analysis—All values are expressed as means ± standard deviation (S.D.). Statistical significance was evaluated using the Student's *t* test with significance accepted when $p < 0.05$. All experiments were performed at least in triplicates.

RESULTS

PMA-induced Monocyte Differentiation Results in Transient YB-1 Phosphorylation—Recently, we described the impact of YB-1 in the course of monocytic cell differentiation (17). To assess whether the posttranslational modification of YB-1 changes during this process, we analyzed the presence of YB-1 and (phosphorylated) p-YB-1 in cell lysates obtained at different time points during PMA-induced differentiation of monocytic THP-1 cells (26). In Western blot analysis, we used a polyclonal anti-YB-1 antibody that specifically detects YB-1 at its phosphorylated serine residue 102 (p-YB-1^{S102}), which is located within the highly conserved cold-shock domain. After 6 h of PMA incubation, we observed enhanced expression of phosphorylated YB-1. Furthermore, an approxi-mately 30 kDa phosphorylated YB-1 fragment appeared at that time point in both the cytoplasm and the nucleus, which tapered off in the subsequent observation period until 48 h (Fig. 1*A*). Of note, in contrast to p-YB-1^{S102}, total YB-1 protein was still detectable 48 h following PMA challenge (Fig. 1*A*, *second row*) pointing to a reversible process. Phosphorylation was prevented to a high degree by preincubation with the phosphoinositide 3-kinase inhibitor Ly294002 in the nuclear compartment (Fig. 1*B*, *upper panel*, *right*). In contrast, there was no effect of Ly294002 on cytoplasmic YB-1 (Fig. 1*B*, *upper panel*, *left*). To analyze subcellular localization of Akt following the differentiation process, we used cytoplasmic and nuclear protein extracts of untreated and PMA-challenged THP-1 cells and analyzed them for Akt protein content by Western blotting. Unchanged Akt protein amounts could be detected in the cytoplasm following PMA challenge, whereas nuclear Akt was enhanced (Fig. 1*C*). In contrast to Ly294002, pre-incubation with SL0101, an inhibitor of p90 ribosomal S6 kinase (RSK), effectively prevented the phosphorylation of YB-1 in both compartments following PMA treatment (Fig. 1*D*).

To confirm phosphorylation and fragmentation of YB-1 following differentiation, primary human monocytes were isolated from healthy blood donors, pooled, and cytoplasmic and nuclear protein extracts thereof were analyzed by Western blot.

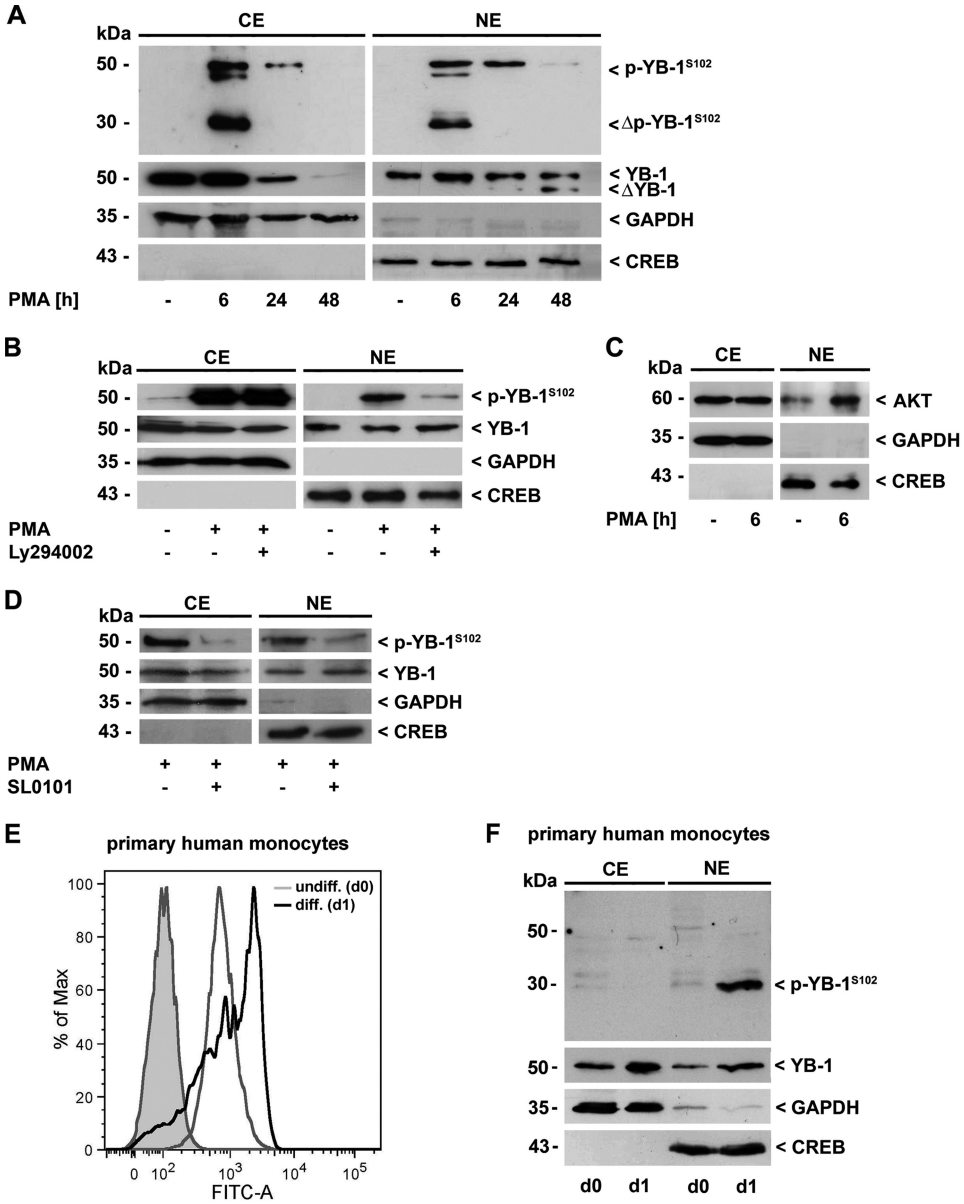

FIGURE 1. **YB-1 is transiently phosphorylated at Ser-102 in the course of monocyte differentiation.** *A*, cytoplasmic (*CE*) and nuclear proteins (*NE*) of THP-1 cells were analyzed for p-YB-1^{S102} and total YB-1 content by Western blot analysis. Fragmentation and transient phosphorylation of YB-1 occurred in the course of PMA-induced monocyte differentiation (100 nM). *B*, YB-1 phosphorylation in the nucleus was effectively prevented by inhibition of the PI3K/Akt signaling pathway by Ly294002 (10 μM). *C*, following PMA challenge (6 h), an enhanced presence of Akt in the nucleus was observed. *D*, inhibition of RSK by SL0101 resulted in reduced p-YB-1^{S102} content in both cytoplasm and nucleus. *E*, differentiation process of human primary monocytes was monitored by enhanced ICAM-1/CD54 expression as a macrophage marker molecule through FACS analysis. *F*, enhanced p-YB-1^{S102} content and fragmentation was observed in CE/NE of primary human monocytes (pooled from three healthy individuals for each experiment) during serum-induced differentiation. Successful separation of cell compartments and equal protein loading were ensured by determining GAPDH and CREB levels. The immunoblot is a representative from three independent experiments.

YB-1 and p-YB-1^{S102} levels were determined in freshly isolated cells and compared with cells that had been incubated for 24 h with human serum to induce differentiation toward a macrophage-like phenotype. Successful differentiation process was monitored by enhanced ICAM-1/CD54 expression (Fig. 1*E*). As observed in THP-1 cells, we detected increased levels of total YB-1 in both, cytoplasm and nuclei of differentiated primary human monocytes. Furthermore, we observed a phosphorylated, ~30 kDa YB-1 fragment in the nuclei of monocytes upon serum incubation. A representative immunoblot from three independent experiments is shown in Fig. 1*F*). Taken together, data from the differentiated primary human monocytes clearly accord with those obtained from the PMA/THP-1 differentiation model, underscoring the physiological relevance of our findings.

Phosphorylation of YB-1 Leads to Enhanced Binding to the CCL5 Promoter—Having demonstrated a YB-1 phosphorylation during monocyte differentiation, we next determined, whether Ser-102 phosphorylation directly influences YB-1-binding affinity to a well-known YB-1 target gene promoter, namely the *CCL5* promoter. In previous studies, we were able to map a specific YB-1-binding motif in the very proximal promoter region (17). ChIP analyses in naive and PMA-activated THP-1 cells using antibodies against YB-1 and p-YB-1^{S102} con-

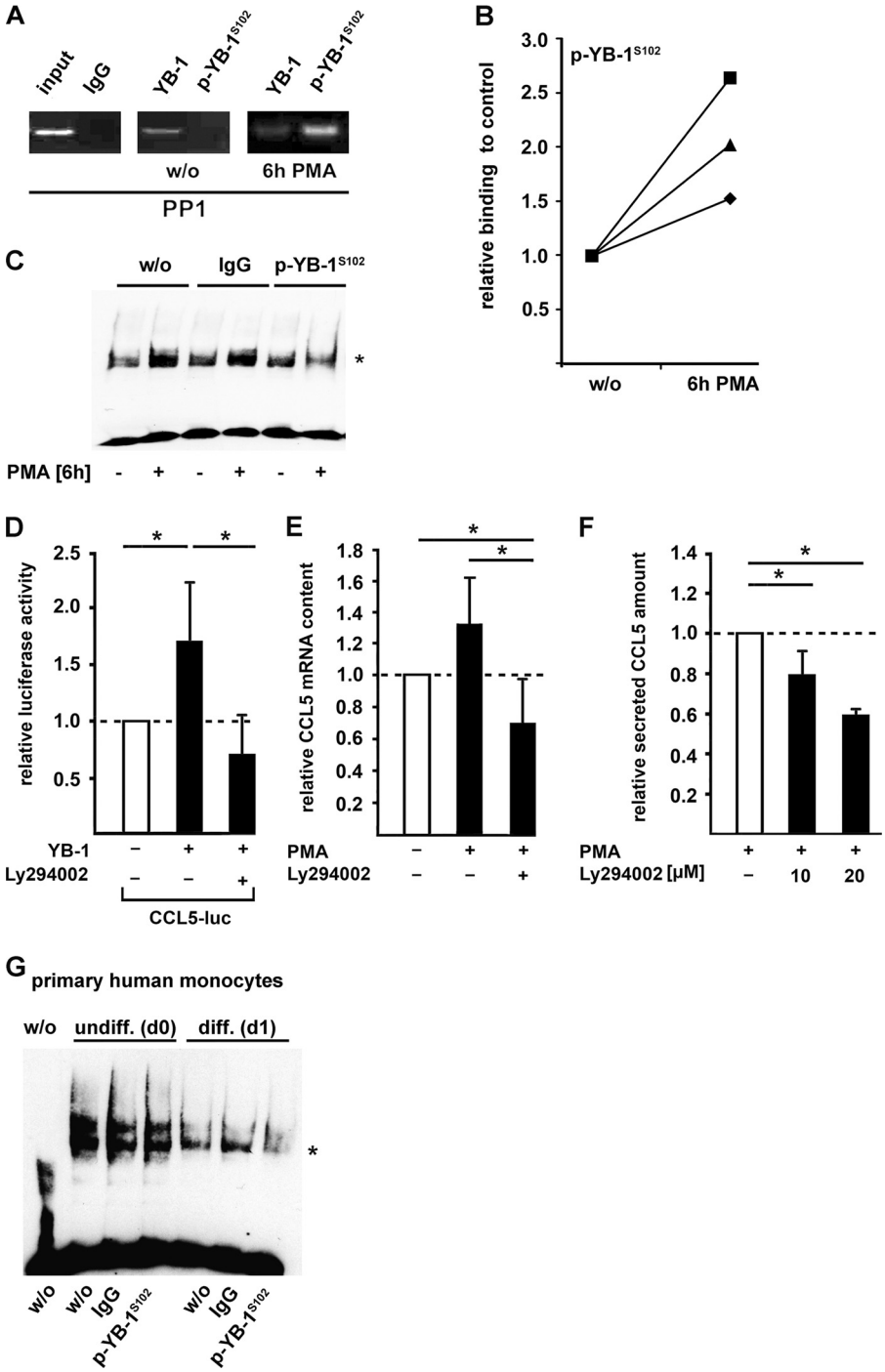

FIGURE 2. **Phosphorylation of YB-1 at Ser-102 increases its binding affinity to *CCL5* promoter region and CCL5 expression in monocytes (THP-1 cells).** *A*, ChIP assays were performed in THP-1 cells incubated with PMA for 6 h using p-YB-1^{S102}-specific antibody or unspecific IgG (negative control). The amount of included DNA was tested without preceding immunoprecipitation (input). *B*, protein-DNA binding from *A* was quantified and confirmed by qRT-PCR in three independent experiments. *C*, EMSA analyses were performed with the antisense Y-box region within the human *CCL5* promoter including nuclear protein extracts from THP-1 cells previously incubated with PMA (100 nM, 6 h) or left untreated. Participation of p-YB-1^{S102} in the complex formation was confirmed by supershift analyses (*) using a p-YB-1^{S102}-specific or nonspecific IgG-antibody as control. *D*, *CCL5* promoter activity was determined in THP-1 cells transfected with a plasmid harboring the proximal 1014 bp of the 5′ regulatory sequence covalently coupled to luciferase reporter gene and with a plasmid encoding for empty vector, wt-YB-1, respectively. Prior to PMA stimulation (100 nM, 6 h), THP-1 cells were preincubated with Akt inhibitor Ly294002 (10 μM) or vehicle for 2 h before *CCL5* promoter activation. CCL5 mRNA (*E*) and secretion (*F*) was assessed by TaqMan and ELISA technology, respectively. Values were normalized to control transfection. Experiments were performed in at least three independent experiments, each performed in triplicate. Data are expressed as mean values ± S.D. *G*, EMSA analyses were performed with the antisense Y-box region within the human *CCL5* promoter including nuclear protein extracts from human primary monocytes previously incubated with human serum for 24 h or left untreated. Participation of p-YB-1^{S102} in the complex formation was confirmed by supershift analyses (*) using a p-YB-1^{S102}-specific or nonspecific IgG antibody as control.

firmed *in vivo* binding of YB-1 to this site (Fig. 2*A*). Beyond that, it proved that binding of serine-phosphorylated YB-1 to this site is strongly enhanced following PMA challenge of THP-1 cells (Fig. 2, *A* and *B*). To confirm the binding of phosphorylated YB-1 to the *CCL5* promoter in PMA-challenged THP-1 cells, we performed electrophoretic mobility supershift assays with an anti-p-YB-1^{S102} antibody. A weaker signal due to size enlargement of the YB-1:DNA complex was only observed in the presence of anti-p-YB-1^{S102} antibody using nuclear extracts of PMA-stimulated THP-1 cells, but neither in extracts of unstimulated cells nor in the presence of unspecific IgG that was included as a negative control (Fig. 2*C*). This indicates that p-YB-1^{S102} binding to the *CCL5* promoter is enhanced in PMA-differentiated monocytes.

Because overexpression of YB-1 in THP-1 cells leads to significantly increased *CCL5* promoter activity (17), we next questioned whether targeting Akt/PKB kinase activity affects YB-1-triggered *CCL5* promoter induction. Preincubation of transfected THP-1 cells with the Akt kinase inhibitor Ly294002 resulted in a complete blockade of the effect triggered by YB-1 over-expression (Fig. 2*D*). This was confirmed at the *CCL5* mRNA and protein levels (Fig. 2, *E* and *F*).

To approve binding of phosphorylated YB-1 to *CCL5* promoter in primary human monocytes, we started the differentiation process by serum incubation for 24 h. Nuclear protein extracts of these cells were analyzed for their binding capacities to the *CCL5* promoter. Supershift analyses demonstrated that p-YB-1^{S102} is included in the DNA:protein complex, whereas an unspecific IgG did not affect the complex intensity (Fig. 2*G*).

Overexpression of CN Reduces p-YB-1 with Consequences for CCL5 Gene Expression—Given that PMA incubation of THP-1 cells resulted in the phosphorylation of YB-1 in a transient manner (see Fig. 1*A*), we hypothesized that an active dephosphorylation process occurs following cell stimulation. Previous studies demonstrated an effect of the CN inhibitor CsA on YB-1 in rMCs (8). Conversely, we speculated that CN itself could dephosphorylate YB-1. To prove this hypothesis, we overexpressed GFP-tagged CN and quantified p-YB-1^{S102} levels in different cell lines. Enhanced CN expression in rMCs (Fig. 3*A*) and in THP-1 cells (Fig. 3*B*) resulted in a more than half-maximal reduction of YB-1 phosphorylation while the total amount of YB-1 did not change under these conditions nor did the control protein GAPDH. Next, we analyzed the CN effects on YB-1-induced target gene expression. Addition of CN diminished p-YB-1^{S102} binding affinity to the *CCL5* promoter, as demonstrated by ChIP analyses (Fig. 3*C*). Along this line, YB-1 increased *CCL5* promoter activity in THP-1 cells (Fig. 3*D, middle bar*) as demonstrated previously (17), whereas co-expression of CN resulted in a complete reversal of this effect (Fig. 3*D, black bar*). Furthermore, a comparable reduction of YB-1-triggered CCL5 expression due to CN over-expression was seen at the mRNA (Fig. 3*E, black bars*) and protein levels with a significant reduction of secreted CCL5 protein after 24 h (Fig. 3*F, black bars*). Effective CN transfection and expression was verified on the mRNA level (Fig. 3*G*). Since we speculate that the YB-1 dephosphorylation upon monocyte differentiation occurs in the nucleus, we assessed whether PMA stimulation of THP-1 cells influences subcellular CN localization. In non-stimulated cells, CN was predominantly localized in the cytoplasm (Fig. 3*H*). However, upon differentiation, CN disappeared in the cytoplasm with the simultaneous appearance in the nucleus (Fig. 3*H*). Thus, 24 h after starting PMA treatment, CN content in the cytoplasm was decreased, but strongly enhanced in the nucleus.

In the next step, we examined a direct participation of CN in the high-molecular weight complex that is formed during monocyte differentiation at the *CCL5* promoter (21). Forty-eight hours following PMA challenge, the introduction of anti-CN antibodies into EMSA reactions resulted in a disappearance of the high-molecular size protein-DNA complex (Fig. 3*I, last lane* and *arrowhead*), whereas neither the anti-phospho-specific YB-1 antibody nor unspecific IgG influenced this complex. In contrast, at 24 h of PMA treatment, the binding of both p-YB-1^{S102} and CN to the smaller complex (** in Fig. 3*I*) could be demonstrated by supershift experiments (Fig. 3*I*).

CN Binds to and Dephosphorylates YB-1—To prove a direct protein-protein interaction between YB-1 and CN, we performed co-immunoprecipitation experiments in HEK293T cells. Since phosphorylated YB-1 was only traceable following extended exposure of the immunoblots, we decided to enhance the p-YB-1^{S102} levels in these cells by pre-incubation with growth factors that had been demonstrated to induce YB-1 phosphorylation at Ser-102 in human breast cancer cells (27). Indeed, epidermal growth factor (EGF) and insulin-like growth factor (IGF) significantly increased the amount of p-YB-1^{S102} in HEK293 cells (Fig. 4*A, lanes 2* and *3*). Next, we examined the CN effect on phosphorylated YB-1. Comparable to rMCs and THP-1 cells, overexpression of CN resulted in a marked reduction of p-YB-1^{S102} in HEK293T cell lysates (Fig. 4*B*, *last lane*).

Using HEK293T cells that overexpressed YB-1 and GFP-tagged CN, we confirmed a direct interaction of YB-1 and CN by co-immunoprecipitation studies. Cell lysates of transfected HEK293T cells were probed with a polyclonal antibody directed against CN or an irrelevant control IgG. Efficient YB-1 protein co-immunoprecipitation with the anti-CN antibody was detected solely when cells were co-transfected with a GFP-CN plasmid (Fig. 4*C*, *lane 6*). In cells expressing GFP protein alone (*lane 5*), or when nonspecific IgG was used for precipitation (*lane 3*), no YB-1 band appeared. To confirm the specificity of this interaction, we assessed whether endogenous YB-1 binds to CN comparably to the overexpressed protein. To enable a longer exposure time of Western blots with reduced unspecific background, we introduced an additional washing step of protein precipitates with PBS. Hereby, we were able to visualize co-immunoprecipitated endogenous YB-1 with the anti-CN antibody in contrast to nonspecific IgG (Fig. 4*D*, *lanes 2* and *1*, *respectively*). As expected, the amount of precipitated YB-1 protein was enhanced when CN was co-expressed (Fig. 4*D*, *lane 4*). To analyze whether the phosphorylation state of YB-1 modulates the interaction with CN, we forced this post-translational modification by incubating the cells with IGF that is known to result in Akt-mediated phosphorylation of YB-1 on Ser-102 (Fig. 4*A*, *lane 3*) (28). Fig. 4*D*, *lane 6* shows that a mildly increased YB-1 phosphorylation results in an enhanced amount of co-immunoprecipitated YB-1 following incubation with the anti-CN antibody. In contrast, no protein-protein interaction

was observed with the control IgG antibody (Fig. 4*D*, *lanes 1*, *3*, and *5*).

In a next step, we assessed the cell compartment of YB-1-CN interaction using cytoplasmic and nuclear protein extracts of HEK293T cells. CN-co-immunoprecipitated endogenous YB-1 was nearly exclusively detected in nuclear protein extracts (Fig. 4*E*, *lanes 6* and *8*), and exceedingly in those cells that were pre-stimulated with IGF (Fig. 4*E*, *lane 8*). A minor amount of YB-1 that co-immunoprecipitated in the cytoplasmic compartment was solely detectable following extended exposure of the immunoblot (data not shown). No YB-1 protein was precipitated with nonspecific IgG (Fig. 4*E*, *lanes 1*, *3*, *5*, and *7*). To prove whether incubation of HEK293T cells with IGF results not only in YB-1 phosphorylation but also in enhanced presence of YB-1 in the nucleus, we performed immunofluorescence of YB-1-CFP-transfected cells with and without IGF stimulation. Following IGF stimulation, an enhanced number of transfected cells displayed YB-1-CFP in the nuclear compart-

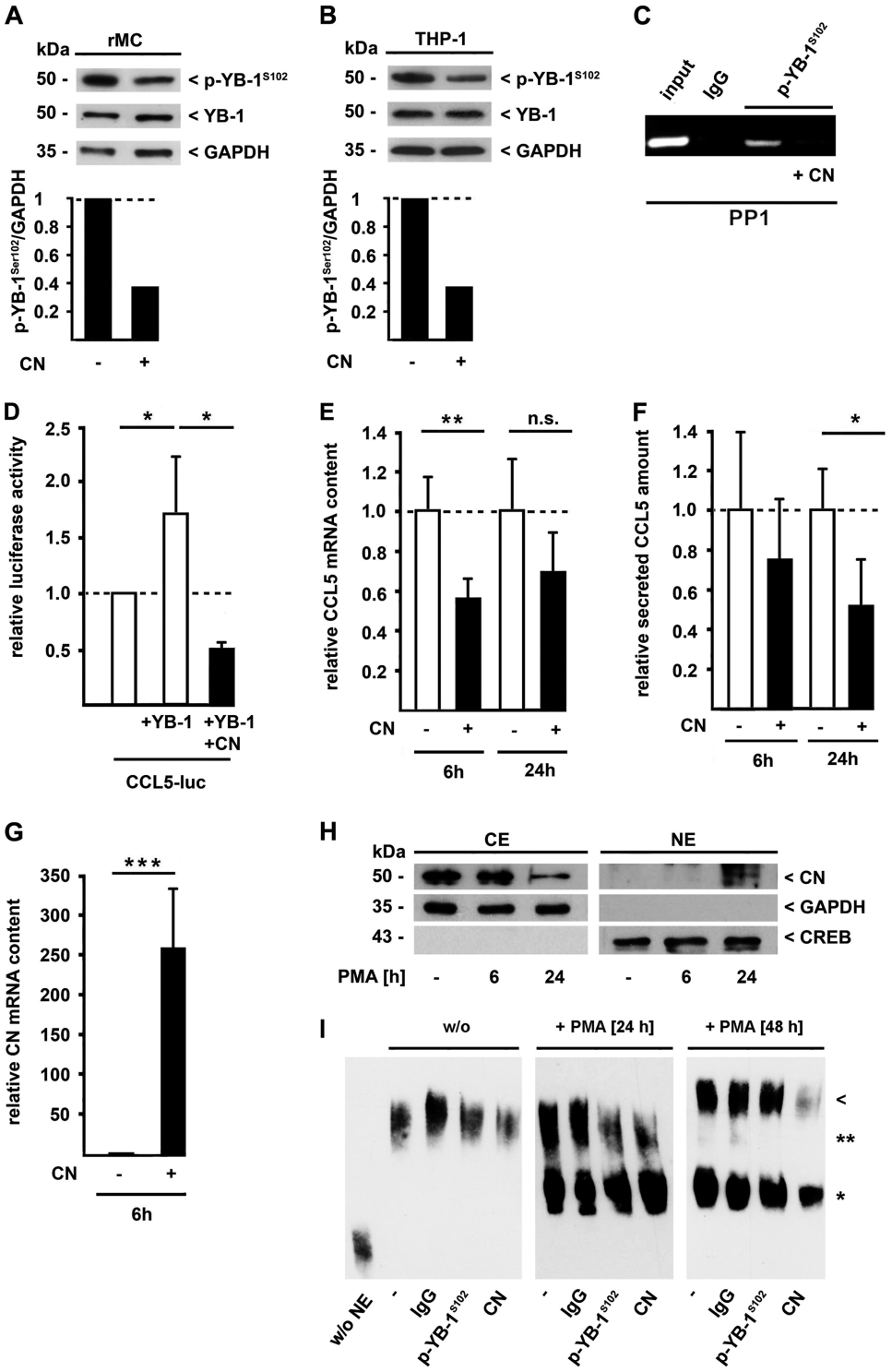

ment (Fig. 4*F*, *lower panels*) whereas in unstimulated cells YB-1-CFP was mainly located in the cytoplasm (Fig. 4*F*, *upper panels*). Taken together, phosphorylation and nuclear translocation of YB-1 in HEK293T cells is induced in response to extracellular stimuli such as IGF, and these processes enhance the direct physical interaction of YB-1 with CN.

In Vivo Inhibition of CN Results in Enhanced YB-1 Phosphorylation in the Kidney—To analyze CN-dependent effects on YB-1 *in vivo*, we examined YB-1 phosphorylation in the presence of the CN inhibitor CsA in BL/6 mice. Mice were injected with CsA (Sandimmune®) for 5 weeks following a one-week low-salt diet. The kidneys were obtained, and Western blot analyses of renal extracts from cytoplasmic and nuclear compartments were performed. In contrast to samples from control animals that received only the solvent, the content of p-YB-1^{S102} was strongly elevated in the nuclear compartment following CsA challenge (Fig. 5).

DISCUSSION

In this study, we demonstrate in both, primary human monocytes and a monocytic cell line, that the differential regulation of *CCL5* gene expression during monocyte/macrophage differentiation highly depends on the phosphorylation status of YB-1. Furthermore, we identified YB-1 as a novel partnering protein of phosphatase CN.

Expression, subcellular localization, and regulatory activities of YB-1 are tightly controlled by several mechanisms including phosphorylation processes that are accomplished by kinases such as Akt/PKB and p90 ribosomal S6 kinase (RSK) (14, 27). During the differentiation of human primary and cell line monocytic cells, p-YB-1^{S102} was detectable in both the cytoplasmic and the nuclear compartment. While RSK activity could be localized to both compartments, Akt/PKB-mediated phosphorylation predominantly occurred in the nucleus, as demonstrated in our studies by interventions with specific kinase inhibitors. In line with this, an enhanced presence of Akt/PKB in the nucleus occurred following PMA-triggered differentiation. It is well documented that Akt/PKB-mediated phosphorylation of YB-1 at Ser-102 in the cytoplasm reduces the ability of YB-1 to bind to the capped 5′-end of mRNA and inhibits cap-dependent translation (29). This process forces nuclear YB-1 translocation (13, 28, 30) and constitutes a prerequisite for downstream signaling events in the nucleus, such as DNA binding and gene regulation. In accordance, loss-of-function mutations at YB-1^{S102} prevent growth induction and nuclear trafficking (28). However, upon monocyte differentiation, only a transient phosphorylation of YB-1 emerged. This was a first indication that a subsequent dephosphorylation process by a phosphatase may additionally modulate YB-1 function. We recently demonstrated that the immunosuppressive drug CsA, a potent inhibitor of the phosphatase CN, induces a strong up-regulation of YB-1 in mesangial cells. This turned out to be dependent on MAPK/ERK and PI3K/Akt pathways, as specific kinase inhibitors counteracted CsA-initiated effects on YB-1 (8). These data are now reinforced by our *in vivo* findings in a model of CsA-triggered fibrosis, where an enhanced p-YB-1^{S102} content was located specifically in nuclei obtained from renal cells (Fig. 5).

There is increasing evidence that YB-1 has an important regulatory role in various inflammatory diseases, such as allergic asthma (31), transplant rejection (17), atherosclerosis (18), sepsis, and sterile inflammation (16). In previous studies, our group identified YB-1 as a cell-type-specific regulator of the chemokine CCL5 (17, 18), a key chemotactic factor for immune cell infiltration. From studies with gelatinase A (32) and GM-CSF (33) genes it is known that YB-1 may act as transcriptional activator and repressor of the same gene, depending on the cellular context. Along this line, on the one hand YB-1 activates CCL5 expression in monocytes, but upon differentiation of these cells to macrophages, YB-1 exhibits a *trans*-repressive effect on the *CCL5* promoter. Thereby, YB-1 drives the early phase of inflammation and additionally contributes to its termination through the shutdown of CCL5 expression upon cell differentiation at later stages. The appearance of a high mobility complex in DNA binding studies indicates that partnering with other transcription factors/cofactors occurs and most likely mediates the repressive effect on gene transcription (17, 21). In our present study, we demonstrate that YB-1 directly interacts with phosphatase CN and that the binding of CN to YB-1 predominantly occurs in the nucleus, as only minor amounts of the CN-YB-1 complex were present in the cytoplasmic fractions. The phosphorylation of YB-1 is increased in response to IGF, and as a consequence thereof, YB-1 shuttles into the nucleus. Furthermore, these processes enhance the interaction of YB-1 with CN. In general, CN accomplishes multiple functions in cells through dephosphorylation of its substrates (NFAT, cdk-4, GABA) (34–36). A nuclear translocation of CN in a

FIGURE 3. **CN-mediated dephosphorylation of p-YB-1^{S102} decreases CCL5 expression in monocytes (THP-1 cells).** Rat mesangial (rMCs) (*A*) or THP-1 cells (*B*) were transfected with a CN-GFP expression plasmid or control vector, and cell lysates were analyzed for p-YB-1^{S102} and total YB-1 content by immunoblot analyses. Densitometric analyses were performed on p-YB-1^{S102} bands with normalization against values determined for GAPDH. Relative band intensities are depicted in bar diagrams *below*. *C*, ChIP assays were performed in THP-1 cells transfected with a CN-GFP expression plasmid or control vector. Four hours after transfection, cells were incubated with PMA for 1 h, and ChIP was performed using a p-YB-1^{S102}-specific antibody or unspecific IgG (negative control) with oligos within the *CCL5* promoter region. The amount of included DNA was tested without preceding immunoprecipitation (input). *CCL5* promoter activity (*D*), *CCL5* mRNA (*E*), and CCL5 protein secretion (*F*) were determined in THP-1 cells transfected with a CN-GFP expression plasmid or control vector. The cellular YB-1 content was manipulated by transfection of THP-1 cells with YB-1-pSG5 expression plasmid (*D*). Cells were harvested 6 or 24 h after transfection and CCL5 mRNA (*E*) and secretion (*F*) was measured by TaqMan and ELISA technology, respectively, and normalized to control transfection. *G*, overexpression of CN was confirmed by TaqMan analysis of THP-1 cells transfected with the CN-GFP expression vector. *H*, Western blot analyses of cytoplasmic (*CE*) and nuclear proteins (*NE*) of THP-1 cells in the course of PMA-induced monocyte differentiation. Compartmental localization of CN was assessed using a specific polyclonal antibody. Separation of cell compartments and equal protein loading were ensured by GAPDH and CREB levels. *I*, nuclear protein extracts from THP-1 cells prior to incubation for 24 or 48 h with PMA or left untreated were prepared and complex formation with the antisense element of the CCL5 promoter was assessed. A strong high-mobility nucleoprotein complex appeared after 48 h of PMA-induced differentiation, which was not detected in the presence of a CN-specific polyclonal antibody (*arrowhead*) but with a p-YB-1^{S102}-specific or nonspecific IgG-antibody as control. Experiments were performed in at least three independent experiments, each performed in triplicate. Data are expressed as mean values ± S.D. *NE*, nuclear extract.

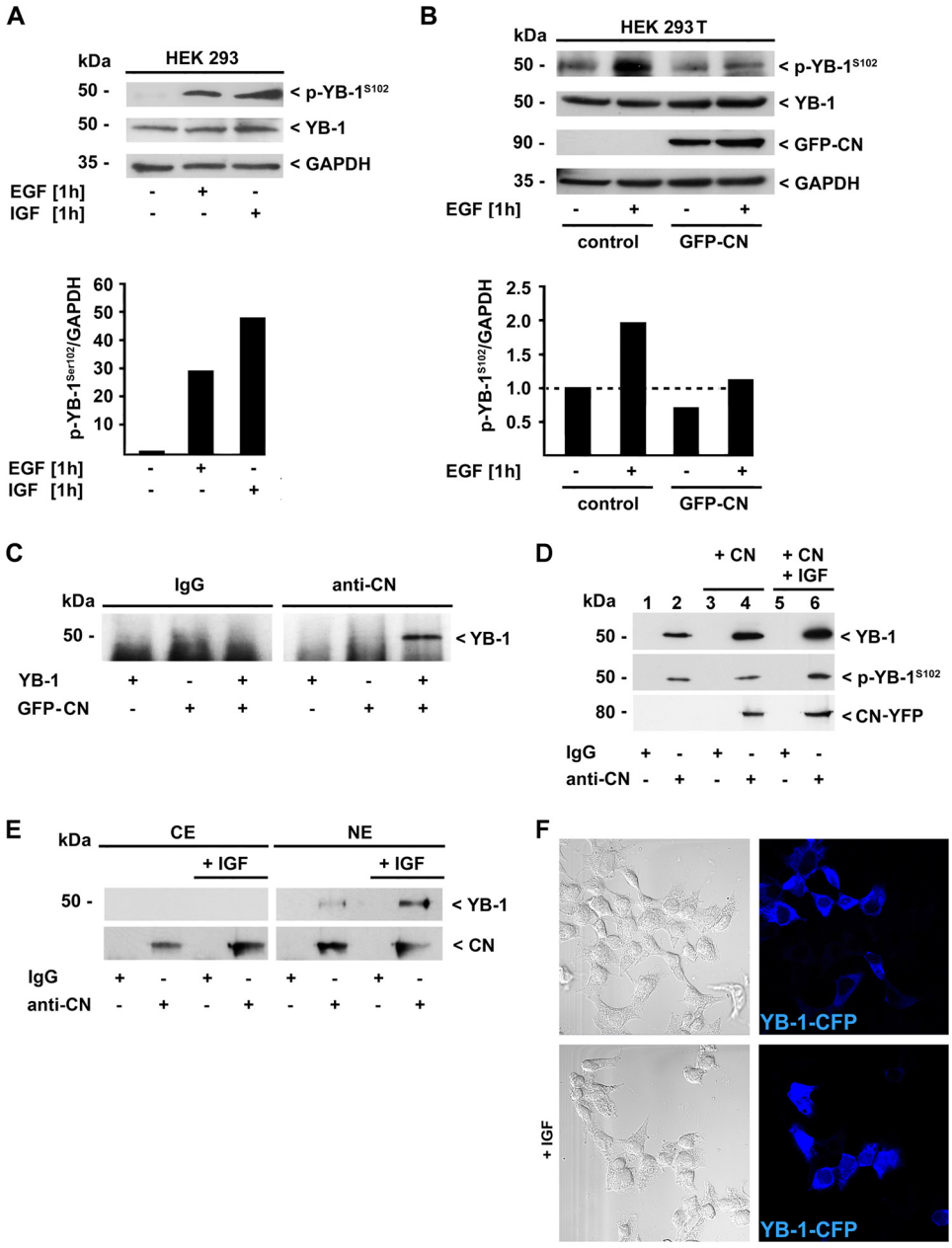

FIGURE 4. **Physical interaction of YB-1 and CN is influenced by the phosphorylation of YB-1 at Ser-102.** *A*, HEK293T cells were treated with 100 ng/ml epidermal (*EGF*), or insulin-like growth factor (*IGF*) and p-YB-1^{S102} and total YB-1-protein content was determined by immunoblot analysis, whereas GAPDH detection ensured equal protein loading. Densitometric analyses were performed with normalization against the GAPDH signals. Relative band intensities are depicted in the histogram below. *B*, HEK293T cells were transfected with a CN-GFP expression plasmid or control vector and stimulated with EGF or vehicle for 1 h. Direct physical interaction of YB-1 with CN was demonstrated in whole cell lysates of HEK293T cells co-transfected with pSG5-YB-1 and CN-GFP (*C*) or transfected with CN-YFP expressing plasmids and stimulated with 100 ng/ml IGF for 1 h (*D*) by immunoprecipitation using a polyclonal anti-CN antibody or unspecific IgG as control. Co-immunoprecipitated YB-1 protein was visualized by Western blot analysis using antibodies raised against the C terminus of YB-1 and against p-YB-1^{S102}. *E*, physical interaction of endogenous YB-1 and CN was analyzed in cytoplasmic and nuclear extracts of HEK293T cells stimulated with 100 ng/ml IGF for 1 h by immunoprecipitation using a polyclonal anti-CN antibody or unspecific IgG as control. Co-immunoprecipitated YB-1 protein was visualized by Western blot analysis using a polyclonal anti-YB-1 antibody raised against the C terminus. *F*, confocal immunofluorescence analysis of YB-1-CFP (*blue*) expressing HEK293T cells stimulated with 100 ng/ml rat IGF for 1 h. Results are representative of three independent experiments.

complex with the transcription factor NFAT has already been shown, whereby CN continues to dephosphorylate NFAT, thereby ensuring the functional activities of this transcriptional regulator (22). In contrast to NFAT, however, CN-mediated dephosphorylation at Ser-102 leads to a deactivation of YB-1 with impact on binding to and regulation of the *CCL5* promoter. Thus, transient overexpression of CN, co-localization and direct protein-protein interaction between CN and YB-1 result in a reduced amount of phosphorylated YB-1 and finally attenuated *CCL5* promoter activity. In accordance with our data, it has been previously shown that the YB-1-binding capacities to the epidermal growth factor receptor (EGFR) promoter depend on the phosphorylation at Ser-102 (37). We demonstrate that a transient upregulation and phosphorylation of YB-1 occurs at the onset of the inflammatory response, whereas YB-1 dephosphorylation *via* CN constitutes a crucial mecha-

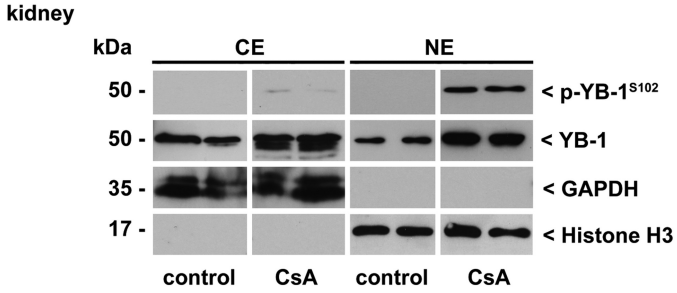

FIGURE 5. **p-YB-1^{S102} content is increased in nuclear extracts of kidneys of CsA-treated mice.** Immunoblotting of cytoplasmic and nuclear kidney protein extracts from mice 5 weeks after daily injection of CsA (30 mg/kg body weight) in comparison with vehicle-injected animals as control. P-YB-1^{S102} and total YB-1 content was assessed by Western blot analyses using a polyclonal anti-p-YB-1^{S102} or anti-YB-1 antibody raised against the C terminus. Separation of cell compartments and equal protein loading were ensured by determining GAPDH and histone H3 levels.

nism that allows for a role of YB-1 in the resolution of inflammation at later stages.

Acknowledgments—We thank Esther Stüttgen for technical assistance. We thank P. Nelson (Division of Clinical Biochemistry, University Hospital, LMU Munich, Munich, Germany) for the donation of the CCL5 reporter construct (38) and O. Ritter (Department of Internal Medicine I, University Hospital, Würzburg, Germany) and M.L. Dell'Acqua and W.A. Sather for CN expression plasmids (Department of Pharmacology University of Colorado School of Medicine, Aurora, CO) (39). We thank G. Müller-Newen (RWTH Aachen University) and the IZKF core unit 'Imaging' for use and advice with the confocal laser-scanning microscope.

REFERENCES

1. Nardozzi, J. D., Lott, K., and Cingolani, G. (2010) Phosphorylation meets nuclear import: a review. *Cell Commun. Signal* **8,** 32
2. Seo, J., and Lee, K. J. (2004) Post-translational modifications and their biological functions: proteomic analysis and systematic approaches. *J. Biochem. Mol. Biol.* **37,** 35–44
3. Jain, J., McCaffrey, P. G., Miner, Z., Kerppola, T. K., Lambert, J. N., Verdine, G. L., Curran, T., and Rao, A. (1993) The T-cell transcription factor NFATp is a substrate for calcineurin and interacts with Fos and Jun. *Nature* **365,** 352–355
4. Rao, A., Luo, C., and Hogan, P. G. (1997) Transcription factors of the NFAT family: regulation and function. *Annu. Rev. Immunol.* **15,** 707–747
5. Burke, B. A., Chavers, B. M., Gillingham, K. J., Kashtan, C. E., Manivel, J. C., Mauer, S. M., Nevins, T. E., and Matas, A. J. (1995) Chronic renal allograft rejection in the first 6 months posttransplant. *Transplantation* **60,** 1413–1417
6. Hariharan, S., Johnson, C. P., Bresnahan, B. A., Taranto, S. E., McIntosh, M. J., and Stablein, D. (2000) Improved graft survival after renal transplantation in the United States, 1988 to 1996. *N. Engl. J. Med.* **342,** 605–612
7. Mihatsch, M. J., Kyo, M., Morozumi, K., Yamaguchi, Y., Nickeleit, V., and Ryffel, B. (1998) The side-effects of ciclosporine-A and tacrolimus. *Clin. Nephrol.* **49,** 356–363
8. Hanssen, L., Frye, B. C., Ostendorf, T., Alidousty, C., Djudjaj, S., Boor, P., Rauen, T., Floege, J., Mertens, P. R., and Raffetseder, U. (2011) Y-Box Binding Protein-1 Mediates Profibrotic Effects of Calcineurin Inhibitors in the Kidney. *J. Immunol.* **187,** 298–308
9. Mertens, P. R., Alfonso-Jaume, M. A., Steinmann, K., and Lovett, D. H. (1999) YB-1 regulation of the human and rat gelatinase A genes via similar enhancer elements. *J. Am. Soc. Nephrol.* **10,** 2480–2487
10. En-Nia, A., Yilmaz, E., Klinge, U., Lovett, D. H., Stefanidis, I., and Mertens, P. R. (2005) Transcription factor YB-1 mediates DNA polymerase α gene expression. *J. Biol. Chem.* **280,** 7702–7711
11. Raffetseder, U., Frye, B., Rauen, T., Jürchott, K., Royer, H. D., Jansen, P. L., and Mertens, P. R. (2003) Splicing factor SRp30c interaction with Y-box protein-1 confers nuclear YB-1 shuttling and alternative splice site selection. *J. Biol. Chem.* **278,** 18241–18248
12. Chen, C. Y., Gherzi, R., Andersen, J. S., Gaietta, G., Jürchott, K., Royer, H. D., Mann, M., and Karin, M. (2000) Nucleolin and YB-1 are required for JNK-mediated interleukin-2 mRNA stabilization during T-cell activation. *Genes Dev.* **14,** 1236–1248
13. Sinnberg, T., Sauer, B., Holm, P., Spangler, B., Kuphal, S., Bosserhoff, A., and Schittek, B. (2012) MAPK and PI3K/AKT mediated YB-1 activation promotes melanoma cell proliferation which is counteracted by an autoregulatory loop. *Exp. Dermatol.* **21,** 265–270
14. Wu, J., Stratford, A. L., Astanehe, A., and Dunn, S. E. (2007) YB-1 is a Transcription/Translation Factor that Orchestrates the Oncogenome by Hardwiring Signal Transduction to Gene Expression. *Transl. Oncogenomics* **2,** 49–65
15. Allemand, E., Hastings, M. L., Murray, M. V., Myers, M. P., and Krainer, A. R. (2007) Alternative splicing regulation by interaction of phosphatase PP2Cγ with nucleic acid-binding protein YB-1. *Nat. Struct. Mol. Biol.* **14,** 630–638
16. Hanssen, L., Alidousty, C., Djudjaj, S., Frye, B. C., Rauen, T., Boor, P., Mertens, P. R., van Roeyen, C. R., Tacke, F., Heymann, F., Tittel, A. P., Koch, A., Floege, J., Ostendorf, T., and Raffetseder, U. (2013) YB-1 Is an Early and Central Mediator of Bacterial and Sterile Inflammation *In Vivo*. *J. Immunol.* **191,** 2604–2613
17. Raffetseder, U., Rauen, T., Djudjaj, S., Kretzler, M., En-Nia, A., Tacke, F., Zimmermann, H. W., Nelson, P. J., Frye, B. C., Floege, J., Stefanidis, I., Weber, C., and Mertens, P. R. (2009) Differential regulation of chemokine CCL5 expression in monocytes/macrophages and renal cells by Y-box protein-1. *Kidney Int.* **75,** 185–196
18. Krohn, R., Raffetseder, U., Bot, I., Zernecke, A., Shagdarsuren, E., Liehn, E. A., van Santbrink, P. J., Nelson, P. J., Biessen, E. A., Mertens, P. R., and Weber, C. (2007) Y-box binding protein-1 controls CC chemokine ligand-5 (CCL5) expression in smooth muscle cells and contributes to neointima formation in atherosclerosis-prone mice. *Circulation* **116,** 1812–1820
19. Wilson, H. M., Walbaum, D., and Rees, A. J. (2004) Macrophages and the kidney. *Curr Opin. Nephrol. Hypertens* **13,** 285–290
20. Shi, C., and Simon, D. I. (2006) Integrin signals, transcription factors, and monocyte differentiation. *Trends Cardiovasc. Med.* **16,** 146–152
21. Raffetseder, U., Liehn, E. A., Weber, C., and Mertens, P. R. (2012) Role of cold shock Y-box protein-1 in inflammation, atherosclerosis and organ transplant rejection. *Eur. J. Cell Biol.* **91,** 567–575
22. Shibasaki, F., Price, E. R., Milan, D., and McKeon, F. (1996) Role of kinases and the phosphatase calcineurin in the nuclear shuttling of transcription factor NF-AT4. *Nature* **382,** 370–373
23. Hallhuber, M., Burkard, N., Wu, R., Buch, M. H., Engelhardt, S., Hein, L., Neyses, L., Schuh, K., and Ritter, O. (2006) Inhibition of nuclear import of calcineurin prevents myocardial hypertrophy. *Circ. Res.* **99,** 626–635
24. MacDonald, G. H., Itoh-Lindstrom, Y., and Ting, J. P. (1995) The transcriptional regulatory protein, YB-1, promotes single-stranded regions in the DRA promoter. *J. Biol. Chem.* **270,** 3527–3533
25. Rauen, T., Raffetseder, U., Frye, B. C., Djudjaj, S., Mühlenberg, P. J., Eitner, F., Lendahl, U., Bernhagen, J., Dooley, S., and Mertens, P. R. (2009) YB-1 acts as a ligand for Notch-3 receptors and modulates receptor activation. *J. Biol. Chem.* **284,** 26928–26940
26. Tsuchiya, S., Kobayashi, Y., Goto, Y., Okumura, H., Nakae, S., Konno, T., and Tada, K. (1982) Induction of maturation in cultured human monocytic leukemia cells by a phorbol diester. *Cancer Res.* **42,** 1530–1536
27. Stratford, A. L., Fry, C. J., Desilets, C., Davies, A. H., Cho, Y. Y., Li, Y., Dong, Z., Berquin, I. M., Roux, P. P., and Dunn, S. E. (2008) Y-box binding protein-1 serine 102 is a downstream target of p90 ribosomal S6 kinase in basal-like breast cancer cells. *Breast Cancer Res.* **10,** R99
28. Sutherland, B. W., Kucab, J., Wu, J., Lee, C., Cheang, M. C., Yorida, E., Turbin, D., Dedhar, S., Nelson, C., Pollak, M., Leighton Grimes, H., Miller, K., Badve, S., Huntsman, D., Blake-Gilks, C., Chen, M., Pallen, C. J., and Dunn, S. E. (2005) Akt phosphorylates the Y-box binding protein 1 at Ser102 located in the cold shock domain and affects the anchorage-inde-

pendent growth of breast cancer cells. *Oncogene* **24,** 4281–4292
29. Evdokimova, V., Ruzanov, P., Anglesio, M. S., Sorokin, A. V., Ovchinnikov, L. P., Buckley, J., Triche, T. J., Sonenberg, N., and Sorensen, P. H. (2006) Akt-mediated YB-1 phosphorylation activates translation of silent mRNA species. *Mol. Cell. Biol.* **26,** 277–292
30. Basaki, Y., Hosoi, F., Oda, Y., Fotovati, A., Maruyama, Y., Oie, S., Ono, M., Izumi, H., Kohno, K., Sakai, K., Shimoyama, T., Nishio, K., and Kuwano, M. (2007) Akt-dependent nuclear localization of Y-box-binding protein 1 in acquisition of malignant characteristics by human ovarian cancer cells. *Oncogene* **26,** 2736–2746
31. Capowski, E. E., Esnault, S., Bhattacharya, S., and Malter, J. S. (2001) Y box-binding factor promotes eosinophil survival by stabilizing granulocyte-macrophage colony-stimulating factor mRNA. *J. Immunol.* **167,** 5970–5976
32. Mertens, P. R., Alfonso-Jaume, M. A., Steinmann, K., and Lovett, D. H. (1998) A synergistic interaction of transcription factors AP2 and YB-1 regulates gelatinase A enhancer-dependent transcription. *J. Biol. Chem.* **273,** 32957–32965
33. Diamond, P., Shannon, M. F., Vadas, M. A., and Coles, L. S. (2001) Cold shock domain factors activate the granulocyte-macrophage colony-stimulating factor promoter in stimulated Jurkat T cells. *J. Biol. Chem.* **276,** 7943–7951
34. Baksh, S., DeCaprio, J. A., and Burakoff, S. J. (2000) Calcineurin regulation of the mammalian G0/G1 checkpoint element, cyclin-dependent kinase 4. *Oncogene* **19,** 2820–2827
35. Garcia-Cozar, F. J., Okamura, H., Aramburu, J. F., Shaw, K. T., Pelletier, L., Showalter, R., Villafranca, E., and Rao, A. (1998) Two-site interaction of nuclear factor of activated T cells with activated calcineurin. *J. Biol. Chem.* **273,** 23877–23883
36. Wang, J., Liu, S., Haditsch, U., Tu, W., Cochrane, K., Ahmadian, G., Tran, L., Paw, J., Wang, Y., Mansuy, I., Salter, M. M., and Lu, Y. M. (2003) Interaction of calcineurin and type-A GABA receptor γ 2 subunits produces long-term depression at CA1 inhibitory synapses. *J Neurosci.* **23,** 826–836
37. Stratford, A. L., Habibi, G., Astanehe, A., Jiang, H., Hu, K., Park, E., Shadeo, A., Buys, T. P., Lam, W., Pugh, T., Marra, M., Nielsen, T. O., Klinge, U., Mertens, P. R., Aparicio, S., and Dunn, S. E. (2007) Epidermal growth factor receptor (EGFR) is transcriptionally induced by the Y-box binding protein-1 (YB-1) and can be inhibited with Iressa in basal-like breast cancer, providing a potential target for therapy. *Breast Cancer Res.* **9,** R61
38. Boehlk, S., Fessele, S., Mojaat, A., Miyamoto, N. G., Werner, T., Nelson, E. L., Schlöndorff, D., and Nelson, P. J. (2000) ATF and Jun transcription factors, acting through an Ets/CRE promoter module, mediate lipopolysaccharide inducibility of the chemokine RANTES in monocytic Mono Mac 6 cells. *Eur. J. Immunol.* **30,** 1102–1112
39. Oliveria, S. F., Dell'Acqua, M. L., and Sather, W. A. (2007) AKAP79/150 anchoring of calcineurin controls neuronal L-type Ca^{2+} channel activity and nuclear signaling. *Neuron* **55,** 261–275